



Title	Structural Transformation of Pt–Ni Nanowires as Oxygen Reduction Electrocatalysts to Branched Nanostructures during Potential Cycles
Author(s)	Kato, Masaru; Iguchi, Yoshimi; Li, Tianchi; Kato, Yuta; Zhuang, Yu; Higashi, Kotaro; Uruga, Tomoya; Saida, Takahiro; Miyabayashi, Keiko; Yagi, Ichizo
Citation	ACS Catalysis, 12(1), 259-264 https://doi.org/10.1021/acscatal.1c04597
Issue Date	2022-01-07
Doc URL	http://hdl.handle.net/2115/87476
Rights	This document is the Accepted Manuscript version of a Published Work that appeared in final form in ACS Catalysis, copyright © American Chemical Society after peer review and technical editing by the publisher. To access the final edited and published work see https://pubs.acs.org/articlesonrequest/AOR-HVAXE3MUU2D9C4M6QGQ9 .
Type	article (author version)
Additional Information	There are other files related to this item in HUSCAP. Check the above URL.
File Information	cs1c04597_si_001.pdf (Supporting information)



[Instructions for use](#)

Supporting information

Structural Transformation of Pt–Ni Nanowires as Oxygen Reduction Electrocatalysts to Branched Nanostructures during Potential Cycles

Masaru Kato,^{*,1,2} Yoshimi Iguchi,² Tianchi Li,² Yuta Kato,² Yu Zhuang,² Kotaro Higashi,³ Tomoya Uruga,^{3,4} Takahiro Saida,⁵ Keiko Miyabayashi,⁶ Ichizo Yagi^{*,1,2}

¹Faculty of Environmental Earth Science, Hokkaido University, N10W5, Kita-ku, Sapporo 060-0810, Japan

²Graduate School of Environmental Science, Hokkaido University, N10W5, Kita-ku, Sapporo 060-0810, Japan

³Innovation Research Center for Fuel Cells, The University of Electro-Communications, Chofugaoka, Chofu, Tokyo 182-8585, Japan

⁴Japan Synchrotron Radiation Research Institute, SPring-8, Sayo, Hyogo 679-5198, Japan

⁵Department of Applied Chemistry, Meijo University, Nagoya 468-8502, Japan

⁶Graduate School of Integrated Science and Technology, Shizuoka University, 3-5-1, Naka-ku, Hamamatsu, Shizuoka, 432-8561, Japan

E-mail: masaru.kato@ees.hokudai.ac.jp (to MK); iyagi@ees.hokudai.ac.jp (to IY)

Experimental section

Materials.

Ethanol, cyclohexane, 2-propanol, perchloric acid, oleylamine, D(+)-glucose and 5% Nafion DE520 were purchased from Wako Pure Chemical Industries, Ltd. [Pt(acac)₂] and Pt/C (TEC10V30E) was purchased from Tanaka Kikinzoku Kogyo. Hexadecyltrimethylammonium chloride (CTAC), [Mo(CO)₆] and [Ni(acac)₂] were commercially available from TCI, Kanto Chemical and Sigma-Aldrich, respectively. Pure oxygen gas (99.995%, Air Liquide Japan), pure argon gas (99.9995%, Hokkaido Air Water) and CO gas (99.9%, GL Science) were used for electrochemical measurements.

Preparation of Pt–Ni nanowires.

Pt–Ni nanowires were prepared in a modified synthetic procedure based on reported synthetic procedures.¹⁻² In 5 mL of oleylamine (15 mmol) in a two-necked round bottom flask (100 mL), 10 mg of [Pt(acac)₂] (0.025 mmol), 6.4 mg of [Ni(acac)₂] (0.025 mmol), 10 mg of CTAC (0.031 mmol), 20 mg of [Mo(CO)₆] (0.075 mmol), and 60 mg of D-glucose (0.33 mmol) were added. The dispersion was kept at ca. 298 K in water under ultrasonication for 30 min and then stirred at <343 K under Ar. After ca. 5 min, the solution mixture became transparent and green. The reaction mixture was transferred to a pre-heated oil bath at 433 K and then kept with stirring at 433 K under Ar for 2 h. The reaction mixture was naturally cooled down in the air to room temperature. A solution mixture (ca. 15 mL) of ethanol and cyclohexane (8:2, v/v) was added to the reaction mixture and then the mixture was centrifuged at 9,500 rpm at 298 K for 5 min using a Micro Refrigerated Centrifuge 3700 equipped with an angle rotor AF-5004CA (Kubota Co.). The supernatant was removed, and the isolated product was rinsed with ca. 15 mL of ethanol–cyclohexane solvent mixture (8:2, v/v) for at least five times under centrifugation at 9,500 rpm at 298 K for 5 min to obtain Pt–Ni nanowires (NW_{Ar}), which also contain Pt–Ni@Ni core–shell nanoparticles. The nanowires were stored in ethanol at room temperature until use. Yield: ca. 5 mg.

Pt–Ni nanowires were also prepared under the air. The heat treatment under the air gave the exclusive nanowires (NW_{air} in the main text).

Preparation of Pt–Ni nanowires supported on carbon supports.

Vulcan XC-72 (ca. 2.3 mg) and Pt–Ni nanowires (ca. 1 mg) were dispersed in 15 mL of an ethanol-cyclohexane mixture (1:1, v/v) and then kept in an ice–water mixture under ultrasonication for at least four hours. The composite was centrifuged down at 9500 rpm

at 298 K for 5 min and then rinsed with ca. 15 mL of ethanol–cyclohexane solvent mixture (8:2, v/v) for at least five times under centrifugation at 9,500 rpm at 298 K for 5 min. The composite was stored in a minimum amount of ethanol (ca. 2 mL) at room temperature until use.

Inductively coupled plasma mass spectrometry (ICP–MS).

ICP–MS was performed using an ICP–MS spectrometer 8800 ICP-QQQ (Agilent Technologies). For sample preparation, a catalyst ink or the catalyst film, which was scraped off from the GC electrode after use, was dispersed in aqua regia solution and then the dispersion was stirred at 308 K for at least 24 h. The dispersion was filtered through a membrane filter (13HP045AN, ADVANTEC), and then the filtrate was diluted with Milli-Q water.

Scanning transmission electron microscopy (STEM) and

STEM images were taken at an acceleration voltage of 200 kV using HD-2000 (Hitachi Scientific Instrument). High-angle annular dark field (HAADF)–STEM images and energy dispersive X-ray spectroscopy (EDS) elemental maps were taken using a JEOL JEM-ARM200F instrument at 200 kV.

Electrochemical measurements.

All electrochemical measurements were performed using a conventional three-electrode setup. A potentiostat (HZ-7000, Hokuto Denko) was used to perform cyclic voltammetry (CV) and linear sweep voltammetry (LSV). A rotating disk electrode (RDE) was used as the working electrode. An Ag|AgCl (sat. KCl) electrode with a double junction holder (International chemistry Co., Ltd) and platinum foil were used as the reference electrode and the counter electrode, respectively. Catalyst-modified glassy carbon (GC) was used as the working electrode.

A GC screw (5 mm ϕ , M4, Tokai Carbon Co., Ltd.) or a GC disk (5 mm ϕ , Tokai Carbon Co., Ltd.) was polished with alumina slurry (0.3 μm , Baikalex), followed by alumina slurry (0.05 μm , Baikalex), and then sonicated in acetone and Milli-Q water for at least 5 min each before drop-casting a catalytic ink. To prepare the catalyst ink, 14 mg of the catalyst was dispersed in a mixture of 6 mL of 2-propanol, 19 mL of Milli-Q water, and 100 μL of 5% Nafion DE520 in a 50 mL glass vial in an ice–water mixture under ultrasonication for at least 2 h. The catalyst ink (20 μL) was drop-cast onto the glassy carbon disk that was rotating at 500–700 rpm using an AFMSRX Analytical Rotator and a MSRX Speed Controller (PINE Research Instrumentation) and kept at room

temperature under rotating for ca. 1 h until the ink was dried. For *in situ* XAS measurements, the catalyst-modified GC screws were heated at 418 K for 5 min to increase the adhesion between the GC and the catalyst film.

CVs and LSVs were recorded in an aqueous solution containing 0.1 M HClO₄. The electrolyte solution was purged with argon or oxygen for at least 30 min before electrochemical measurements. For electrochemical cleaning, 100 potential cycles at 200 mV s⁻¹ in the potential range between 0.05 and 1.20 V vs. RHE were performed in a 0.1 M HClO₄ aqueous solution under Ar before collecting CVs and LSVs shown in the main text. All LSVs under oxygen are corrected by the subtraction of the current densities of the corresponding working electrode recorded under Ar. All potentials are shown against the RHE.

For CO stripping measurements, a 0.1 M HClO₄ aqueous electrolyte solution was purged with CO for 10 min and then with Ar for 60 min. A bias potential of 0.05 V vs. RHE was applied to a sample electrode during purging with CO and Ar until the measurements began. Cyclic voltammograms were recorded in the potential range from 0.05 to 1.45 V vs. RHE for two cycles at 50 mV s⁻¹ under Ar. Electrochemically active surface areas based on the desorption of H_{upd} observed in the second cycle and the electrochemical oxidation of CO observed in the first cycle were determined from the difference between the first and second cycles.

The mass activity (MA) of the catalysts was determined at +0.9 V vs. RHE based on the kinetically controlled current density (j_k) obtained in the Koutechy–Levich plot for the ORR and the amount of Pt in the catalyst used on the GC electrode. The amount of Pt was determined by ICP-MS. The specific activity (SA) was determined at +0.9 V vs. RHE based on the j_k and ECSA_{CO}.

XAS measurements.

Pt *L*₃-edge XAS measurements of the as-prepared Pt–Ni NW_{Ar}/C in the transmission method were performed at BL5S1 and BL11S2 stations in AichiSR. Boron nitride (BN) was used to make a pellet containing the sample. Pt *L*₃-edge XAS data were collected using a 21 Ge-element detector in a fluorescent method at BL36XU station in SPring-8.³ For *in situ* measurements, a RDE with a catalyst-modified GC was used as the working electrode in 0.1 M HClO₄ under nitrogen. A platinum foil and a reversible hydrogen (International chemistry Co., Ltd) electrode were used as the counter and reference electrodes, respectively. Electrochemical data were collected using AutoLab Potential

and Galvanostat system (Metrohm). Before *in situ* XAS measurements, 0.1 M HClO₄ aqueous electrolyte solution in a polyether ether ketone (PEEK) cell was purged with nitrogen for at least 30 min, and then 50 potential cycles at 200 mV s⁻¹ were performed in the potential range from 0.05 to 1.0 V vs. RHE under nitrogen for electrochemical cleaning. XANES spectra of the catalysts were obtained at 0.4, 0.7, 0.9, 1.0 and 1.1 V vs. RHE. XANES spectra were normalized using Athena software.⁴

EXAFS oscillation data, $\chi(k)$, were extracted from the XAS data after the background subtraction. The k^3 -weighted EXAFS oscillation data, $k^3\chi(k)$, in the k range from 3 to 12 Å⁻¹ were Fourier-transformed into R -space, followed by the inverse Fourier transform into k -space for curve-fitting analysis using software package REX2000 (Rigaku Co.).⁵⁻⁷

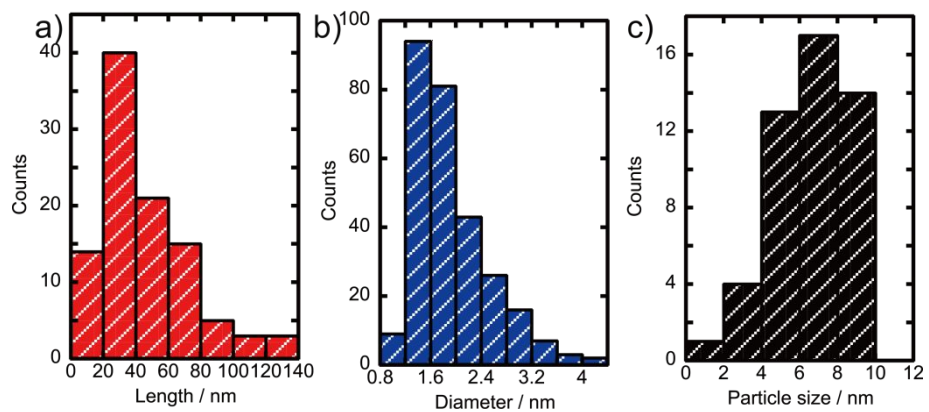


Figure S1. (a) Length and (b) diameter distributions of Pt–Ni NWs and (c) diameter distributions of NPs found in NW_{Ar}/C .

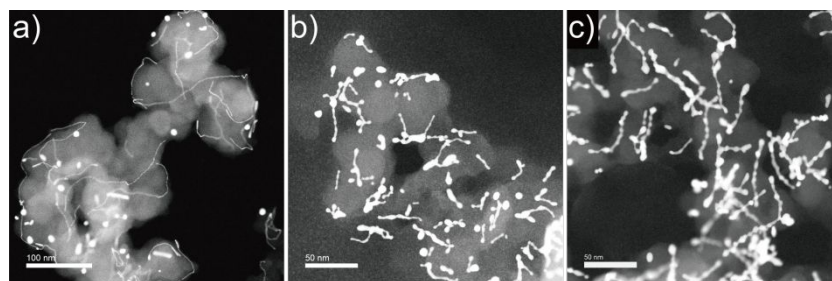


Figure S2. Representative HAADF-STEM images of (a) the as-prepared NW_{Ar}/C, (b) NW_{Ar}/C_25k, and (c) NW_{Ar}/C_50k. HAADF-STEM images including these images allowed us to determine ratios of the number of NWs (and branched structures) and NPs to be 101:101 (1:1) for the as-prepared NW_{Ar}/C, 265:87 (ca. 3:1) for NW_{Ar}/C_25k, and 255:55 (ca. 5:1) for NW_{Ar}/C_50k.

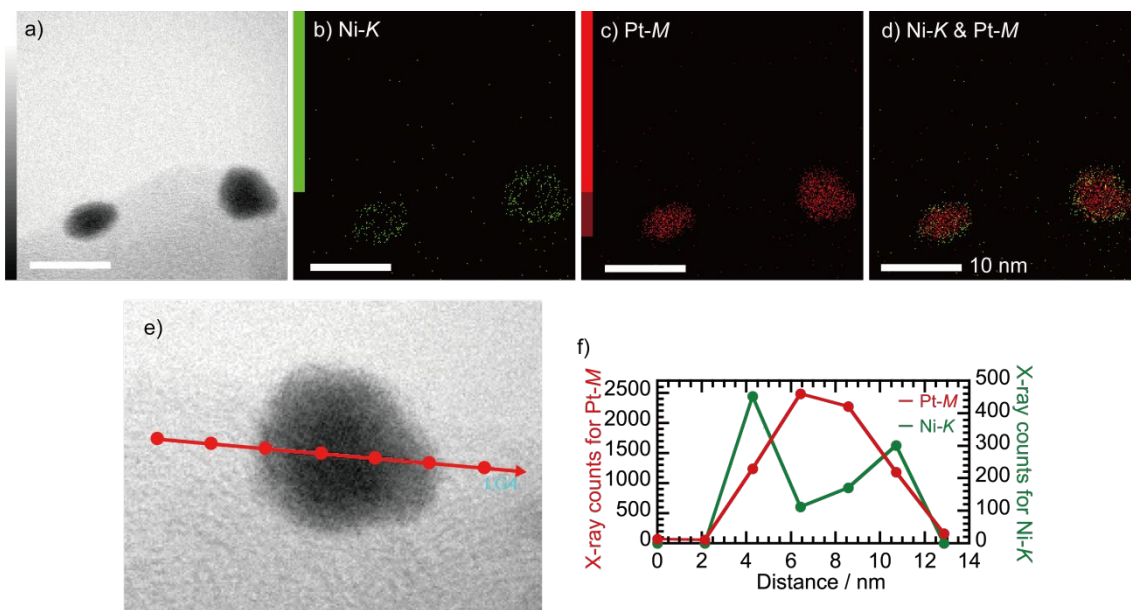


Figure S3. (a) STEM image and EDS maps of carbon-supported Pt-Ni@Ni core-shell NPs, which co-present with NW_{Ar} , for (b) the Ni-K signals in green, (c) the Pt-M signals in red and (d) the overlay of Pt-M and Ni-K signals. (e,f) EDS line profile analysis of NPs at each point (seven points in total) for the Pt-M and Ni-K signals.

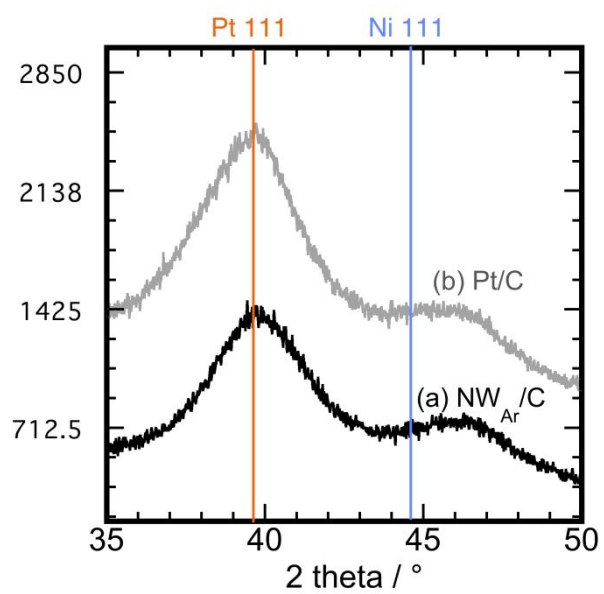


Figure S4. Power X-ray diffraction patterns of (a) the as-prepared Pt–Ni NW_{Ar}/C and (b) Pt/C. The orange and blue lines show the 111 diffraction position for the bulk Pt and Ni, respectively.

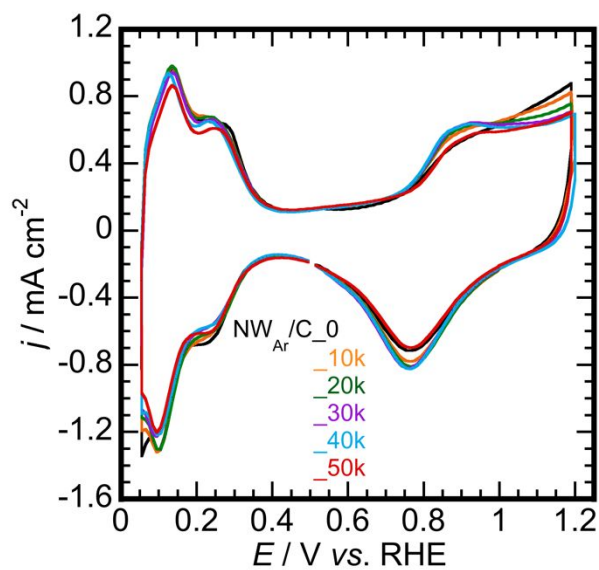


Figure S5. CVs of $\text{NW}_{\text{Ar}}/\text{C}$ recorded at 200 mV s^{-1} in a 0.1 M HClO_4 aqueous solution under Ar before and after potential cycles up to 50k. CVs after 0k (before potential cycles), 10k, 20k, 30k, 40k and 50k potential cycles are shown in black, orange, green, purple, blue and red, respectively.

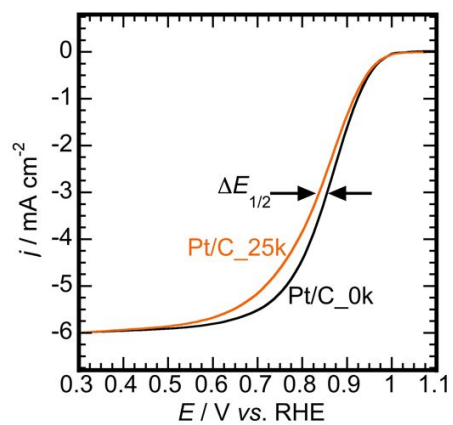


Figure S6. LSVs of Pt/C before (the trace in black) and after 25k potential cycles (the trace in orange). LSVs were recorded at 1600 rpm and 10 mV s^{-1} in a 0.1 M HClO_4 aqueous solution under oxygen.

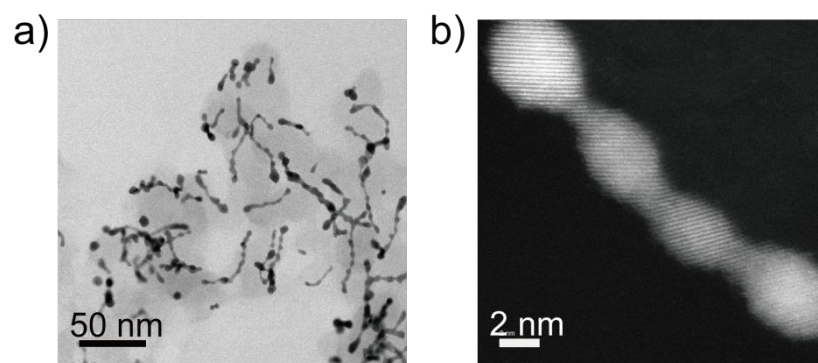


Figure S7. (a) STEM and (b) HAADF-STEM images of Pt-Ni NW_{AT}/C_{50k}.

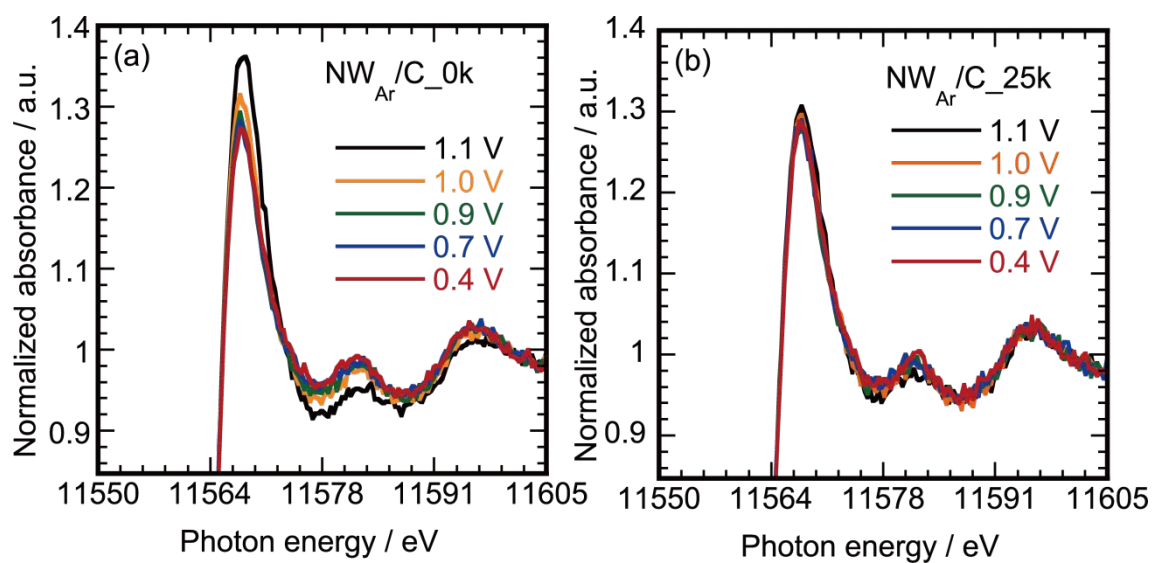


Figure S8. Enlarged potential dependent XANES spectra of (a) NW_{Ar}/C_{0k} and (b) NW_{Ar}/C_{25k} in the Pt L_3 edge white line region.

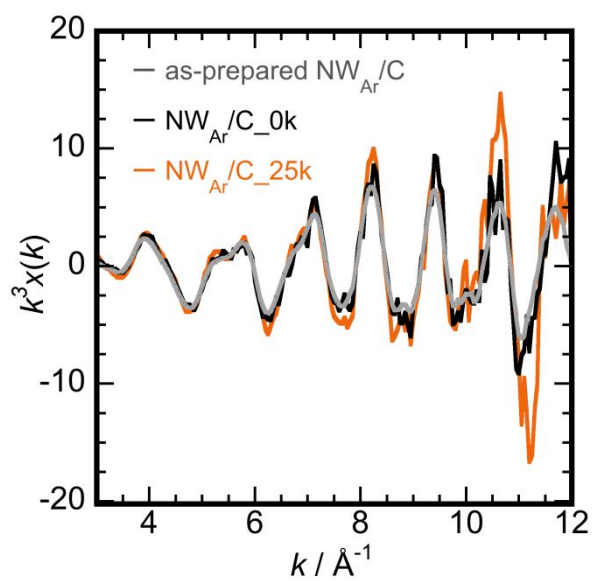


Figure S9. (a) EXAFS oscillation of (a) the as-prepared $\text{NW}_{\text{Ar}}/\text{C}$ collected in the transmission method (the trace in gray) and (b) $\text{NW}_{\text{Ar}}/\text{C}_{0\text{k}}$ (the trace in black) and (c) $\text{NW}_{\text{Ar}}/\text{C}_{25\text{k}}$ (the trace in orange) collected in the fluorescence method.

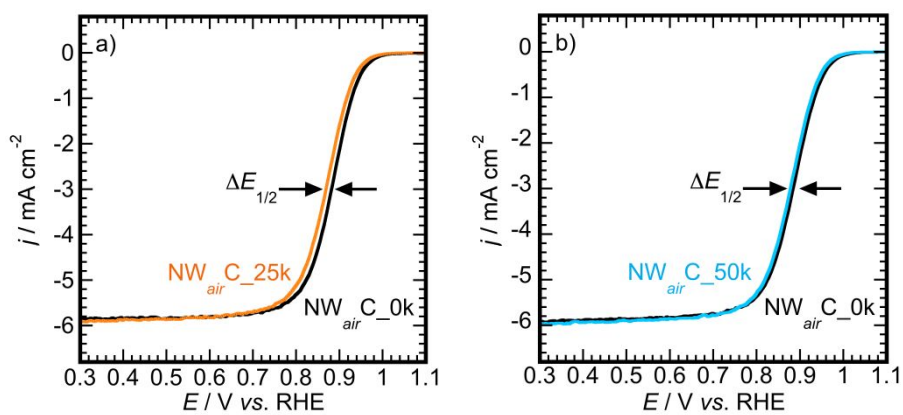


Figure S10. Comparisons of LSVs of Pt–Ni NW_{air}/C_{0k} with (a) NW_{air}/C_{25k} and (b) NW_{air}/C_{50k} recorded at 1600 rpm at 10 mV s^{-1} in a positive-going sweep in a 0.1 M HClO_4 aqueous solution under oxygen.

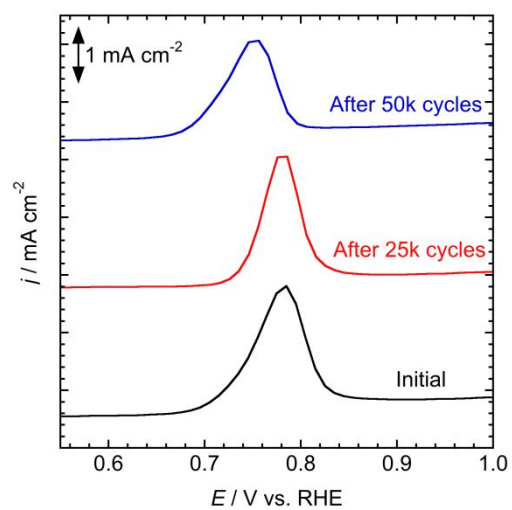


Figure S11. CO stripping voltammograms of $\text{NW}_{air}/\text{C}_{0k}$ (the trace in black), $\text{NW}_{air}/\text{C}_{25k}$ (the trace in red) and $\text{NW}_{air}/\text{C}_{50k}$ (the trace in blue) recorded at 50 mV s^{-1} in a 0.1 M HClO_4 aqueous solution under Ar. The differences between voltammograms recorded at the first and second cycles are shown for each sample.

Table S1. Parameters used for curve-fitting analysis of EXAFS oscillations.

Sample	Data collection method	Coordination number	Pt-Pt distance / Å	ΔE / eV	Debye Waller factor / Å	R / %
As-prepared Pt-Ni NW _{A_r} /C	Transmission	8.8±1.2	2.74±0.01	9.3±1.6	0.080±0.008	4.8
As-prepared Pt-Ni NW _{A_r} /C	Fluorescence	7.0±1.3	2.74±0.01	9.6±2.3	0.055±0.021	6.4
Pt-Ni NW _{A_r} /C_25k	Fluorescence	7.4±1.6	2.73±0.01	6.6±2.6	0.044±0.028	3.8

References

1. Sun, Y.; Luo, M.; Qin, Y.; Zhu, S.; Li, Y.; Xu, N.; Meng, X.; Ren, Q.; Wang, L.; Guo, S. Atomic-Thick PtNi Nanowires Assembled on Graphene for High-Sensitivity Extracellular Hydrogen Peroxide Sensors. *ACS Appl. Mater. Interf.* **2017**, *9*, 34715-34721. DOI: 10.1021/acsami.7b11758.
2. Jiang, K.; Zhao, D.; Guo, S.; Zhang, X.; Zhu, X.; Guo, J.; Lu, G.; Huang, X. Efficient oxygen reduction catalysis by subnanometer Pt alloy nanowires. *Sci. Adv.* **2017**, *3*, e1601705. DOI: 10.1126/sciadv.1601705.
3. Nagasawa, K.; Takao, S.; Nagamatsu, S.-i.; Samjeské, G.; Sekizawa, O.; Kaneko, T.; Higashi, K.; Yamamoto, T.; Uruga, T.; Iwasawa, Y. Surface-Regulated Nano-SnO₂/Pt₃Co/C Cathode Catalysts for Polymer Electrolyte Fuel Cells Fabricated by a Selective Electrochemical Sn Deposition Method. *J. Am. Chem. Soc.* **2015**, *137*, 12856-12864. DOI: 10.1021/jacs.5b04256.
4. Ravel, B.; Newville, M. ATHENA, ARTEMIS, HEPHAESTUS: data analysis for X-ray absorption spectroscopy using IFEFFIT. *J. Synchrotron Radiat* **2005**, *12*, 537-541. DOI: 10.1107/S0909049505012719.
5. Taguchi, T. REX2000 Version 2.5: Improved DATA Handling and Enhanced User-Interface. *AIP Conf. Proc.* **2007**, *882*, 162-164. DOI: 10.1063/1.2644462.
6. Taguchi, T.; Ozawa, T.; Yashiro, H. REX2000 Yet Another XAFS Analysis Package. *Physica Scripta* **2005**, 205. DOI: 10.1238/physica.topical.115a00205.
7. Asakura, K. In *X-Ray Absorption Fine Structure for Catalysts and Surfaces*, pp 33-58.